Radii and binding energies in oxygen isotopes: a puzzle for nuclear forces

V. Lapoux[1],* V. Somà[1], C. Barbieri[2], H. Hergert[3], J. D. Holt[4], and S. R. Stroberg[4]
[1] *CEA, Centre de Saclay, IRFU, Service de Physique Nucléaire, 91191 Gif-sur-Yvette, France*
[2] *Department of Physics, University of Surrey, Guildford GU2 7XH, United Kingdom*
[3] *National Superconducting Cyclotron Laboratory and Department of Physics and Astronomy, Michigan State University, East Lansing, MI 48824, USA and*
[4] *TRIUMF, 4004 Wesbrook Mall, Vancouver, British Columbia, Canada V6T 2A3*
(Dated: May 3, 2016)

We present a systematic study of both nuclear radii and binding energies in (even) oxygen isotopes from the valley of stability to the neutron drip line. Both charge and matter radii are compared to state-of-the-art *ab initio* calculations along with binding energy systematics. Experimental matter radii are obtained through a complete evaluation of the available elastic proton scattering data of oxygen isotopes. We show that, in spite of a good reproduction of binding energies, *ab initio* calculations with conventional nuclear interactions derived within chiral effective field theory fail to provide a realistic description of charge and matter radii. A novel version of two- and three-nucleon forces leads to considerable improvement of the simultaneous description of the three observables for stable isotopes, but shows deficiencies for the most neutron-rich systems. Thus, crucial challenges related to the development of nuclear interactions remain.

PACS numbers: 25.60.-t,21.10.-k,21.10.Jx, 24.10.Eq

Our present understanding of atomic nuclei faces the following major questions. Experimentally, we aim (i) to determine the location of the proton and neutron drip-lines [1, 2], i.e. the limits in neutron numbers N upon which, for fixed proton number Z, with decreasing or increasing N, nuclei are not bound with respect to particle emission, and (ii) to measure nuclear structure observables offering systematic tests of microscopic models. While nuclear masses have been experimentally determined for the majority of known light and medium-mass nuclei [3], measurements of charge and matter radii are typically more challenging. Charge radii for stable isotopes have been accessed in the past by means of electron scattering [4]. In recent years, laser spectroscopy experiments allow extending such measurements to unstable nuclei with lifetimes down to a few milliseconds [5]. Matter radii are determined by scattering with hadronic probes which requires a modelization of the reaction mechanism. Theoretically, intensive works have been performed towards linking a universal description of atomic nuclei to elementary interactions [6, 7] amongst constituent nucleons and ultimately to the underlying theory of strong interactions, Quantum Chromo-Dynamics (QCD). If accomplished, this *ab initio* description would be beneficial both for a deep understanding of known nuclei (stable and unstable, totalling around 3300) and to predict on reliable bases the features of undiscovered ones (few more thousands are expected). Many of the latter are not, in the foreseeable future, experimentally at reach, yet they are crucial to understand nucleosynthesis phenomena, modelled using large sets of evaluated data and of calculated observables.

The reliability of first-principles calculations depends upon a consistent understanding of fundamental observables: ground-state characteristics related to the existence (masses, expressed as binding energies) and sizes (expressed as root mean square - rms - radii). Special interest resides in the study of masses and sizes for a given element along isotopic chains. Experimentally, their determination is increasingly difficult as one approaches the neutron drip-line; as of today, the heaviest element with available data on all existing bound isotopes is oxygen (Z=8) [3]. Theoretically, the link between nuclear properties and inter-nucleon forces can be explored for different N/Z values, thus critically testing both our knowledge of nuclear forces and many-body theories.

In this work, we focus on oxygen isotopes for which, in spite of the tremendous progress of *ab initio* methods over last years, a simultaneous reproduction of masses and radii has not yet been achieved. We present important findings from novel *ab initio* calculations along with a complete evaluation of matter radii, r_m, for stable and neutron-rich oxygen isotopes. Here, r_m are deduced via a microscopic reanalysis of proton elastic scattering data sets. They complement charge radii r_{ch}, offering an extended comparison through the isotopic chain that allows testing state-of-the-art many-body calculations. We show that a recent version of two- and three-nucleon (2N and 3N) forces leads to considerable improvement in the critical description of radii.

A viable *ab initio* strategy consists in exploiting the separation of scales between QCD and (low-energy) nuclear dynamics, taking point nucleons as degrees of freedom and using the principles of effective field theory (EFT). In this context, chiral EFT provides a systematic construction of nuclear forces, a well-founded starting point for structure calculations [6, 7]. Many-body techniques have themselves undergone major progress and extended their domain of applicability both in mass and in terms of accessible (open-shell) isotopes for a given el-

ement [8–19]. An emblematic case that has received considerable attention is oxygen binding energies, where several calculations have established the crucial role played by 3N forces in the reproduction of the neutron drip line at ^{24}O [9, 20–25]. The excellent agreement between experimental data and calculations based on a next-to-next-to-next-to-leading order (N^{3}LO) 2N and N^{2}LO 3N chiral interaction (EM) [26–28] was greeted as a milestone for *ab initio* methods, even though a consistent description of nuclear radii could not be achieved at the same time [29]. Since then, this deficiency has remained a puzzle. Subsequent calculations of heavier systems [10–12] and infinite nuclear matter [30, 31] confirmed the systematic underestimation of charge radii, a sizable overbinding and too spread-out spectra, all pointing to an incorrect reproduction of the saturation properties of nuclear matter. While interactions with good saturation properties existed [32–34], this problem led to the focused development of a novel nuclear interaction, NNLO$_{\rm sat}$ [35], which includes contributions up to N^{2}LO in the chiral EFT expansion (both in 2N and 3N sector) and differs from EM in two main aspects. First, the optimisation of the ("low-energy") coupling constants is performed simultaneously for 2N and 3N terms [36]; EM, in contrast, optimizes 3N forces subsequently. Second, in addition to observables from few-body (A=2,3,4) systems, experimental constraints from light nuclei (energies and charge radii in some C and O isotopes) are included in the optimization. This aspect departs from the strategy of EM, in which parameters in the A-body sector are fixed uniquely by observables in A-body systems. Although first applications point to good predictive power for ground-state properties [35, 37, 38], the performance of the NNLO$_{\rm sat}$ potential remains to be tested along complete isotopic chains.

Here, we employ two different many-body approaches, self-consistent Green's function (SCGF) and in-medium similarity renormalisation group (IM-SRG), each available in two versions. The first are based on standard expansion schemes and thus applicable only to closed-shell nuclei: Dyson-SCGF (DGF) [39] and single-reference IM-SRG (SR-IM-SRG) [40] respectively. The second are built on Bogoliubov-type reference states and thus allow for a proper treatment of pairing correlations and systems displaying an open-shell character. These are labelled Gorkov-SCGF (GGF) [8] and multi-reference IM-SRG (MR-IM-SRG) [9], respectively. For the MR-IM-SRG, the reference state is first projected on good proton and neutron numbers. Having different *ab initio* approaches at hand is crucial to benchmark theoretical results and infer as unbiased as possible information on the input forces. Moreover, while DGF, SR- and MR-IM-SRG feature a comparable content in terms of many-body expansion, GGF currently includes a lower amount of many-body correlations, which allows testing the many-body convergence [10].

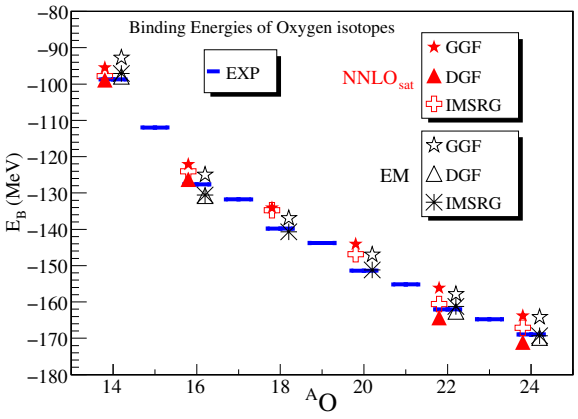

FIG. 1. Oxygen binding energies. Results from SCGF and IMSRG calculations with EM and NNLO$_{\rm sat}$ are displayed along with experimental data.

We first compute binding energies E_B for $^{14-24}$O for the two sets of 2N and 3N interactions with the four many-body schemes. EM is further evolved to a low-momentum scale $\lambda = 1.88 - 2.0\,\mathrm{fm}^{-1}$ by means of SRG techniques [41, 42]. Results are displayed in Fig. 1. For both interactions, different many-body calculations yield values of E_B spanning intervals of up to 10 MeV, from 5 to 10% of the total. Compared to experimental binding energies, EM and NNLO$_{\rm sat}$ perform similarly, following the trend of available data along the chain both in absolute and in relative terms. Overall, results shown in Fig. 1 confirm previous findings for EM and validate the use along the isotopic chain for NNLO$_{\rm sat}$.

We now examine the nuclear charge observables. In addition to r_{ch} radii, analytical forms of fitted experimental charge densities can be extracted from (e,e) cross sections. Standard forms include 2- or 3-parameter Fermi (2pF or 3pF) profiles [43]. By unfolding [44] the finite size of proton charge distribution (whose r_{ch} radius is 0.877(7) fm [45]), proton ground-state (gs) densities can be deduced. It should be underlined that, due to the various analysis techniques providing charge densities, the global systematic error on r_p is significantly larger (roughly 0.05 fm) than the one on single r_{ch} values (of the order of 0.01 fm). For ^{16}O, r_{ch} was estimated to be 2.730 (25) fm [46] and 2.737 (8) fm [43, 47]. Differences in r_{ch} between ^{17,18}O and ^{16}O, $\Delta r_{ch} = -0.008(7)$ and $+0.074(8)$ fm [47], are affected by the same systematic errors.

In this work we determine matter radii via the proton probe. We consider angular distributions of proton elastic scattering cross sections and compare data to calculations performed using a microscopic density-dependent optical potential model (OMP) inserted in the Distorted Wave Born Approximation (DWBA). This type of analysis has been recently successfully applied to the case of helium isotopes, for which r_m radii were extracted with

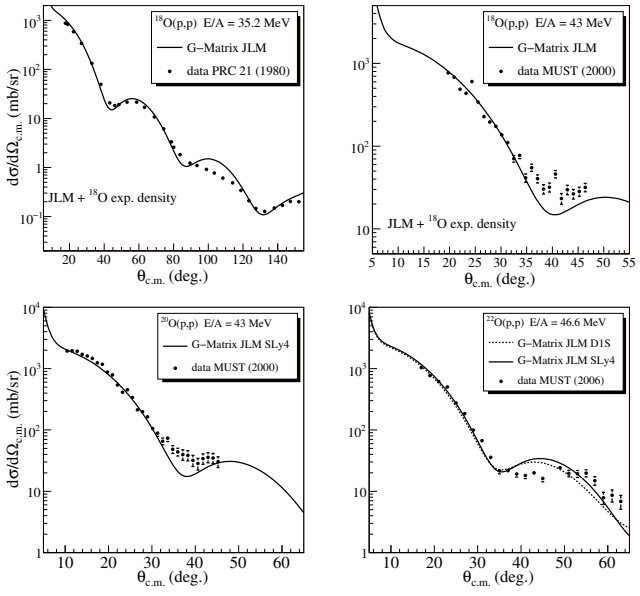

FIG. 2. Experimental elastic (p,p) distributions compared to OMP calculations (*this work*). (Top) ^{18}O (data: [51, 52]). (Bottom) ^{20,22}O (data: [52]).

uncertainties of the order of 0.1 fm [48]. We employ the energy- and density-dependent JLM potential [49], derived from a G-matrix formalism and extensively tested in the analysis of nucleon scattering data for a wide range of nuclei. This complex potential depends only on the incident energy E and on neutron and proton densities. Here we use the standard form $U_{JLM}(\rho, E) = \lambda_V V(\rho, E) + i\lambda_W W(\rho, E)$, with $\lambda_V = \lambda_W = 1$. For $^{18-22}$O, nucleon separation energies are sufficiently high to exclude strong coupling effects to continuum or to excited states, and the imaginary part is enough to include implicitly all other relevant coupled-channel effects.

For the stable symmetric ^{16}O, r_m was extracted from combined (e,e), (p,p) and (n,n) in Ref. [50] using the following procedure: the (3pF) density profile ρ_p was deduced from electron scattering data [46], the same profile was assumed for the neutron density distribution. This "experimental" matter density built from the (e,e) data was used to compute the potentials. This procedure was followed also for ^{17,18}O, with the neutron density profiles initially taken as $(N/Z) * \rho_p$ then adjusted to reproduce elastic data on heavy ions [44]. We refer to densities extracted in this way as the "experimental" ("exp") ones, with r_p values for $^{16-18}$O given in Tab. I.

We first performed OMP calculations for ^{18}O and compared them to data collected at 35.2 A·MeV in direct [51], and at 43 A·MeV in inverse kinematics [52]. Starting from a 2pF profile fitted to "exp" densities, by changing the two parameters governing size and diffusiveness, we generated a family of densities then inserted into the OMP and fitted to data. Since only the most forward angles have small global errors and are sensitive to the size of the nucleus, we limited our fit to 46° and 33° for 35.2 and 43 A·MeV data respectively, i.e. to data with statistical + systematic errors below 10%. By keeping the curves falling within χ^2/d.o.f. < 1, we determined an associated matter radius $r_m = 2.75(10)$ fm. The 2pF profiles with the same r_m lead to very similar χ^2/d.o.f., signaling that calculations, in the region of forward angles, are rather insensitive to the diffusiveness. As shown in Fig. 2, calculations are in good agreement with (p,p) data, which confirms the validity of the OMP approach provided that realistic densities are employed. We repeated the analysis using densities generated by Hartree-Fock BCS calculations [52] with Skyrme interactions, each associated with a different r_m. Results are very similar to the ones of Fig. 2, with $r_m = 2.77(10)$ fm, close to the one from "exp" densities. This validates the use of OMP calculations to estimate r_m radii from (p,p) cross sections [48].

For unstable ^{20,22}O, elastic proton scattering cross sections were measured using oxygen beams at 43 and 46.6 A·MeV respectively [52, 53]. We performed OMP calculations with microscopic densities for ^{20,22}O. Angular distributions up to 30° (for ^{20}O) and 33° (for ^{22}O) were considered for the fits. Results are displayed in Fig. 2. In order to show the sensibility to the microscopic inputs, we compare, for ^{22}O, results with densities from the Sly4 [54] Skyrme interaction with those obtained with densities from Hartree-Fock-Bogoliubov calculations based on the Gogny D1S force [55, 56]. In both cases, (p,p) cross sections are well reproduced. Resulting r_m radii are 2.90 fm in ^{20}O along with 2.96 and 3.03 fm in ^{22}O for Sly4 and D1S densities, respectively. The sensitivity study led us to the same range of ±0.1 fm, which is the uncertainty on our values throughout the (p,p) analysis. The results are summarised in Tab. I.

Studying interaction cross sections (σ_I) [58] is another way of deducing matter radii. In Fig. 3 we compare experimental r_m radii for $^{16-22}$O from (e,e) and (p,p) to values obtained from σ_I measurements [58, 59] (see also Tab. I). While (e,e) and (p,p) provide a consistent set of r_p and r_m radii for $^{16-18}$O, this is not the case for r_m values obtained from σ_I, usually extracted without including correlations in the target, which arguably influences

A	16	17	18	20	22
r_p	2.59 (7)	2.60 (8)	2.68 (10)		
r_m (σ_I)	2.54 (2)	2.59 (5)	2.61 (8)	2.69(3)	2.88(6)
r_m (p,p)	2.60 (8)	2.67 (10)	2.77 (10)	2.9 (1)	3.0 (1)

TABLE I. Experimental rms radii of oxygen isotopes: r_p and r_m evaluated from heavy-ion scattering for $A = 16$, 17 [44] and (p,p) data [50] for $A = 16$; r_p for A=18 from the charge density [57]; r_m from σ_I [58]; for A =18-22, r_m (*this work*) from (p,p) data.

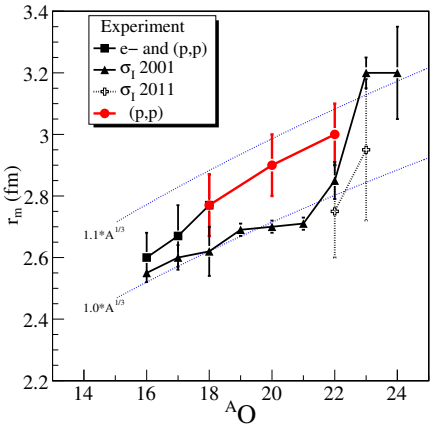

FIG. 3. Experimental values for the r_m radii, deduced from σ_I, (e,e) and (p,p) measurements (see Tab. I). Blue lines show the $A^{1/3}$ behaviour of the liquid drop model.

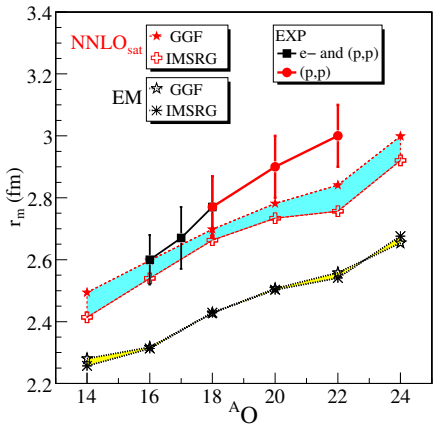

FIG. 5. Matter radii from our analysis and given in Tab. I, compared to calculations with EM [26–28] and NNLO$_{\rm sat}$ [35]. Bands span results from GGF and MR-IMSRG schemes.

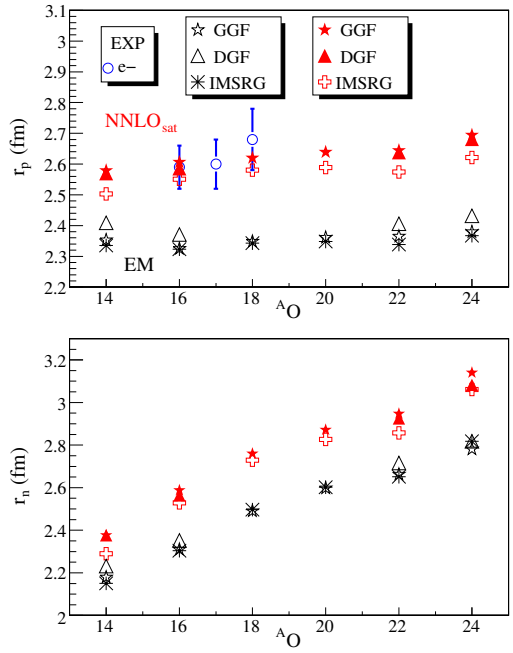

FIG. 4. Proton (top) and neutron (bottom) radii obtained from IM-SRG and SCGF calculations with EM and NNLO$_{\rm sat}$. Experimental r_p values are given in Tab. I.

scattering amplitudes. Since our analysis of the stable isotopes, used as a reference, provides r_m radii with an uncertainty of the order of 0.1 fm, we also conclude that uncertainties deduced from σ_I are underestimated. Consequently, we focus on results obtained from (e,e) and (p,p) data for the comparison with theory.

We start by analyzing calculations for proton and neutron radii, shown in Fig. 4. We notice that, for each interaction, there is good agreement between the various methods, which span 0.05 (0.1) fm when EM (NNLO$_{\rm sat}$) is used. This shows that different state-of-the-art schemes achieve, for a given interaction, an uncertainty that is smaller than (i) experimental ones and (ii) the uncertainty coming from the use of different interactions. Clear discrepancies are observed between radii computed with EM and NNLO$_{\rm sat}$, with the former being systematically smaller by 0.2-0.3 fm. While EM largely underestimates data, r_p values are well reproduced by NNLO$_{\rm sat}$, keeping in mind that r_{ch} of ^{16}O is included in the NNLO$_{\rm sat}$ fit. The performance along the isotopic chain can be seen for matter radii, where in Fig. 5 the evaluations from the (p,p) analysis are compared to GGF and MR-IMSRG. Similar conclusions are drawn by considering other schemes, see Fig. 4. Rms radii computed with EM underestimate evaluated data by about 0.3-0.4 fm for all isotopes. Results significantly improve with NNLO$_{\rm sat}$, although the description deteriorates towards the neutron drip line, with a discrepancy of about 0.2 fm in ^{22}O. Recently, a similar effect was observed for the calcium isotopes [38].

These results reinforce the progress of nuclear *ab initio* calculations, which are able to address systematics of isotopic chains beyond light systems and thus provide critical feedback on the long-term developments of inter-nucleon interactions. To this extent, joint theory-experiment and theory-theory analyses are essential and have to start with a realistic description of both sizes and masses. In this work we focused on the oxygen chain, the heaviest one for which experimental information on both E_B and radii is available up to the neutron drip line. We showed that nuclear sizes of unstable isotopes can be obtained through the (p,p) data analysis within 0.1 fm. The combined comparison of measured charge/matter radii and E_B with *ab initio* calculations offers unique insight on nuclear forces: the current standard EM yields an excellent reproduction of E_B but significantly underestimates radii, whereas the unconventional NNLO$_{\rm sat}$ clearly improves the description of radii. Our results raise ques-

tions about the choice of observables that should be included in the fit and the resulting predictive power whenever this strategy is followed.

More precise information on oxygen radii, e.g. r_{ch} via laser spectroscopy measurements, would allow confirming our (p,p) analysis and further refining the present discussion. Similar studies in heavier isotopes will also contribute to the systematic development of nuclear forces. Finally, we stress that a simultaneous reproduction of binding energies and radii in stable and neutron-rich nuclei is mandatory for reliable structure but even more for reaction calculations. Scattering amplitudes and nucleon-nucleus interactions evolve as a function of the size, which should be consistently taken into account when more microscopic reaction approaches are considered.

ACKNOWLEDGEMENTS

The *Espace de Structure et de réactions Nucléaires Théorique* ESNT (http://esnt.cea.fr) framework at CEA is gratefully acknowledged for supporting the project that initiated the present work. The authors would like to thank T. Duguet for useful discussions and P. Navrátil, A. Calci, S. Binder, J. Langhammer, and R. Roth for providing the interaction matrix elements used in the present calculations. C. B. is funded by the Science and Technology Facilities Council (STFC) under grant No. ST/L005743/1. SCGF calculations were performed by using HPC resources from GENCI-TGCC (Contracts No. 2015-057392 and 2016-057392) and the DiRAC Data Analytic system at the University of Cambridge (under BIS National E-infrastructure grant No. ST/K001590/1 and STFC grants No. ST/H008861/1, ST/H00887X/1 and ST/K00333X/1). H. H. acknowledges support by the NSCL/FRIB Laboratory. TRIUMF receives federal funding via a contribution agreement with the National Research Council of Canada. Computing resources for MR-IM-SRG calculations were provided by the Ohio Supercomputing Center (OSC) and the National Energy Research Scientific Computing Center (NERSC), a DOE Office of Science User Facility supported by the Office of Science of the U.S. Department of Energy under Contract No. DE-AC02-05CH11231.

* E-mail address: vlapoux@cea.fr

[1] J. Erler, N. Birge, M. Kortelainen, W. Nazarewicz, E. Olsen, A. M. Perhac and M. Stoitsov, *The limits of the nuclear landscape*, Nature **486**, 509-512 (2012).
[2] M. Thoennessen, Int. J. Mod. Phys. E **24**, 153002 (2015).
[3] G. Audi, M. Wang, A.H. Wapstra, F.G. Kondev, M. MacCormick, X. Xu, and B. Pfeiffer, Chinese Physics C **36** 1287 (2012).
[4] R. Hofstadter, Rev. Mod. Phys. **28**, 214 (1956).
[5] J. Billowes and P. Campbell, J. Phys. G: Nucl. Part. Phys. **21**, 707 (1995).
[6] E. Epelbaum, H.-W. Hammer, and U.-G. Meißner, Rev. Mod. Phys. **81**, 1773 (2009).
[7] R. Machleidt and D. Entem, Phys. Rep. **503**, 1 (2011).
[8] V. Somà, T. Duguet and C. Barbieri, Phys. Rev. C **84**, 064317 (2011).
[9] H. Hergert, S. Binder, A. Calci, J. Langhammer, and R. Roth, Phys. Rev. Lett. **110**, 242501 (2013).
[10] V. Somà, A. Cipollone, C. Barbieri, P. Navrátil and T. Duguet, Phys. Rev. C **89**, 061301 (2014).
[11] S. Binder, J. Langhammer, A. Calci, and R. Roth, Phys. Lett. B **736**, 119 (2014).
[12] H. Hergert, S. K. Bogner, T. D. Morris, S. Binder, A. Calci, J. Langhammer, and R. Roth, Phys. Rev. C **90**, 041302 (2014).
[13] J. D. Holt, J. Menéndez, and A. Schwenk, Phys. Rev. Lett. **110**, 022502 (2013).
[14] J. D. Holt, J. Menendez, J. Simonis, and A. Schwenk, Phys. Rev. C **90**, 024312 (2014).
[15] G. Hagen, T. Papenbrock, M. Hjorth-Jensen, and D. J. Dean, Rep. Prog. Phys. **77**, 096302 (2014).
[16] S. K. Bogner, H. Hergert, J. D. Holt, A. Schwenk, S. Binder, A. Calci, J. Langhammer, and R. Roth, Phys. Rev. Lett. **113**, 142501 (2014).
[17] G. R. Jansen, J. Engel, G. Hagen, P. Navrátil, and A. Signoracci, Phys. Rev. Lett. **113**, 142502 (2014).
[18] A. Signoracci, T. Duguet, G. Hagen, and G. R. Jansen, Phys. Rev. C **91**, 064320 (2015).
[19] T. Duguet, J. Phys. G: Nucl. Part. Phys. **42**, 025107 (2015).
[20] T. Otsuka, T. Suzuki, J. D. Holt, A. Schwenk, and Y. Akaishi, Phys. Rev. Lett. **105**, 032501 (2010).
[21] G. Hagen, M. Hjorth-Jensen, G. R. Jansen, R. Machleidt, T. Papenbrock, Phys. Rev. Lett. **108**, 242501 (2012).
[22] J. D. Holt, J. Menéndez, and A. Schwenk, Eur. Phys. J. A **49**, 39 (2013).
[23] A. Cipollone, C. Barbieri, and P. Navrátil, Phys. Rev. Lett. **111**, 062501 (2013).
[24] T. A. Lähde, E. Epelbaum, H. Krebs, D. Lee, U.-G. Meißner, and G. Rupak, Phys. Lett. B **732**, 110 (2014).
[25] K. Hebeler, J. D. Holt, J. Menéndez, and A. Schwenk, Ann. Rev. Nucl. Part. Sci. **65**, 457 (2015).
[26] D.R. Entem and R. Machleidt, Phys. Rev. C **68**, 041001 (2003).
[27] P. Navrátil, Few-Body Systems 41, 117 (2007).
[28] R. Roth, S. Binder, K. Vobig, A. Calci, J. Langhammer, and P. Navrátil, Phys. Rev. Lett. **109**, 052501 (2012).
[29] A. Cipollone, C. Barbieri, and P. Navrátil, Phys. Rev. C **92**, 014306 (2015).
[30] A. Carbone, A. Polls, and A. Rios, Phys. Rev. C **88**, 044302 (2013).
[31] G. Hagen, T. Papenbrock, A. Ekström, K. A. Wendt, G. Baardsen, S. Gandolfi, M. Hjorth-Jensen, and C. J. Horowitz, Phys. Rev. C **89**, 014319 (2014).
[32] K. Hebeler, S. K. Bogner, R. J. Furnstahl, A. Nogga, and A. Schwenk, Phys. Rev. C **83**, 031301(R) (2011).
[33] L. Coraggio, J. W. Holt, N. Itaco, R. Machleidt, L. E. Marcucci, and F. Sammarruca, Phys. Rev. C **89**, 044321 (2014).
[34] J. Simonis, K. Hebeler, J. D. Holt, J. Menéndez, and A. Schwenk, Phys. Rev. C **93**, 011302(R) (2016).

[35] A. Ekström, G. R. Jansen, K. A. Wendt, G. Hagen, T. Papenbrock, B. D. Carlsson, C. Forssén, M. Hjorth-Jensen, P. Navrátil, and W. Nazarewicz, Phys. Rev. C **91**, 051301 (2015).
[36] B. D. Carlsson, A. Ekström, C. Forssén, D. F. Strömberg, O. Lilja, M. Lindby, B. A. Mattsson, and K. A. Wendt, (2015), arXiv:1506.02466 [nucl-th].
[37] G. Hagen et al., Nature Phys. 12, 186 (2015).
[38] R. F. Garcia Ruiz et al., Nature Physics AOP, doi:10.1038/nphys3645 (2016).
[39] W. H. Dickhoff and C. Barbieri, Prog. Part. Nucl. Phys. **52**, 377 (2004).
[40] K. Tsukiyama, S. Bogner, and A. Schwenk, Phys. Rev. Lett. **106**, 222502 (2011).
[41] S. K. Bogner, R. J. Furnstahl, and R. J. Perry, Phys. Rev. C **75**, 061001(R) (2007).
[42] S. K. Bogner, R. J. Furnstahl, and A. Schwenk, Prog. Part. Nucl. Phys. **65**, 94 (2010).
[43] H. De Vries, C. W. De Jager, and C. De Vries, At. Data Nucl. Data Tables **36**, 495 (1987), *and ref. therein.*
[44] G. R. Satchler and W. G. Love, Phys. Rept. **55**, 183 (1979).
[45] K. Nakamura *et al.*, Particle Data Group, J. Phys. G **37**, 075021 (2010).
[46] I. Sick and J. S. McCarthy, Nucl. Phys. **A150**, 631 (1970).
[47] H. Miska et al., Phys. Lett. B **83**, 165 (1979).
[48] V. Lapoux and N.Alamanos, Eur. Phys. J. A **51**, 91 (2015).
[49] J.P. Jeukenne, A. Lejeune and C. Mahaux, Phys. Rev. C **16**, 80 (1977).
[50] J.S. Petler *et al.*, Phys. Rev. C **32**, 673 (1985).
[51] E. Fabrici *et al.*, Phys. Rev. C **21**, 844 (1980).
[52] E. Khan *et al.*, Phys. Lett. B. **490**, 45 (2000).
[53] E. Becheva *et al.*, *The MUST collaboration*, Phys. Rev. Lett. **9**6, 012501 (2006).
[54] E. Chabanat, P Bonche, P. Haensel, J. Meyer, R. Schaeffer, Nucl. Phys A **635**, 231 (1998).
[55] J. Dechargé and D. Gogny, Phys. Rev. C **21**, 1568-1593 (1980).
[56] J.-F. Berger, M. Girod, and G. Gogny, Comput. Phys. Commun. 63, 365 (1991).
[57] B. Norum et al., Phys. Rev. C 25, 1778 (1982).
[58] A. Ozawa, T. Suzuki, I. Tanihata, Nucl. Phys. A **693**, 32 (2001).
[59] R. Kanungo *et al.* Phys. Rev. C **84**, 061304 (R) (2011).